IET Microwaves, Antennas & Propagation

WILEY

The Institution of Engineering and Technology

ORIGINAL RESEARCH OPEN ACCESS

Array Antenna Radiation Pattern Synthesis Using Mixture Density Networks With Iterative Retraining

Je-Heon Lee[1] | Hyeon-Chang Seong[1] | Jungsuek Oh[2] | Jae Hee Kim[1]

[1]School of Electrical, Electronics and Communication Engineering, Korea University of Technology and Education, Cheonan, South Korea | [2]New Media and Communications, Department of Electrical and Computer Engineering, Seoul National University, Seoul, South Korea

Correspondence: Jae Hee Kim (jaehee@koreatech.ac.kr)

Received: 19 March 2026 | **Revised:** 19 July 2026 | **Accepted:** 20 July 2026

Keywords: antenna arrays | antenna radiation patterns | learning (artificial intelligence)

ABSTRACT

This paper proposes an artificial intelligence algorithm based on a mixture density network (MDN) to solve the inverse problem of estimating the excitation phases of antenna elements for array antenna radiation pattern synthesis. In array antenna radiation pattern synthesis, a nonuniqueness issue exists in which multiple phase solutions can produce an identical radiation pattern, which limits the effectiveness of conventional deep learning models in learning multiple solutions. The proposed MDN estimates the probability distribution of antenna excitation signals from a target radiation pattern, thereby effectively learning multiple feasible solutions. In addition, an iterative retraining framework based on the error between the target radiation pattern and the predicted radiation pattern is introduced to improve prediction accuracy. Simulation results for an eight-element array antenna demonstrate that the proposed MDN achieves superior phase estimation performance for radiation patterns not included in the training dataset and arbitrarily generated radiation patterns.

1 | Introduction

In recent years, array antennas have been widely used in various applications such as wireless communications and radar systems. Array antennas offer the advantage of enhancing communication efficiency and mitigating coverage shadow regions by enabling the synthesis of radiation patterns with various shapes [1, 2].

To obtain a desired radiation pattern using an array antenna, the excitation phases and amplitudes of individual antenna elements must be properly controlled. When the phase and amplitude of each element are given, the radiation pattern can be readily calculated using the array factor. However, the radiation pattern synthesis problem, which aims to inversely estimate the excitation phases of antenna elements from a given radiation pattern, is computationally challenging and inherently nonunique. This is because the array factor calculated from the excitation phases and amplitudes contains both magnitude and phase information, whereas the radiation pattern provides only magnitude information as a function of angle and does not include phase information. Consequently, a direct mathematical inversion is not feasible.

Various algorithms have been proposed to address this inverse problem. Representative approaches include genetic algorithms (GA) [3], particle swarm optimisation (PSO) [4], and differential evolution algorithms (DEA) [5]. Although these optimisation-based methods are flexible and applicable to a wide range of array antenna configurations, they suffer from high computational costs due to iterative search and evaluation processes as well as unstable convergence behaviour. To overcome these limitations, deep learning-based approaches have recently attracted considerable attention. Studies have been conducted in which artificial neural networks (ANNs) learn the nonlinear mapping between radiation patterns and phase vectors to enable fast prediction [6–9]. Furthermore, ANN frameworks based on encoder–decoder architectures have demonstrated the potential for real-time design by performing phase prediction and radiation pattern analysis in parallel [10, 11]. However, although these approaches perform well for problems with a single output corresponding to a given input, they exhibit limited capability in learning scenarios where multiple phase solutions exist for a single radiation pattern. To address this issue, inverse design methods using generative adversarial networks (GANs) have been proposed for structures such as metasurfaces [12–14]. Nevertheless, GAN-based approaches tend to generate solutions that closely resemble the training data and may produce significantly different results depending on the noise input.

Therefore, this paper proposes the use of a mixture density network (MDN) [15, 16] as a probabilistic learning model to estimate antenna excitation phases in array antenna inverse design problems where multiple outputs correspond to a single input. The MDN predicts multiple feasible solutions in the form of a probability distribution for a given input and probabilistically estimates the phase distribution from the radiation pattern, thereby overcoming the limitations of conventional deep neural network (DNN)-based approaches. Section 2 describes the proposed MDN-based phase estimation method for solving the array antenna inverse problem. Section 3 presents a performance evaluation of the proposed MDN model and a comparative analysis with a conventional DNN. Section 4 introduces an iterative retraining method based on data augmentation to improve prediction accuracy. Finally, Section 5 presents the conclusions.

2 | MDN Structure for Radiation Pattern Synthesis

The theoretical background and structure of the MDN for estimating the excitation phases of an array antenna from a given target radiation pattern are presented, the one-to-many mapping problem (where multiple phase solutions exist for an identical radiation pattern) is analysed based on the mathematical relationship between the antenna signal phase and the radiation pattern, and the specific neural network architecture, input/output variable configuration, and loss function model of the proposed MDN are introduced to overcome the limitations of conventional learning models.

2.1 | Relationship Between Signal Phase and Radiation Pattern of an Array Antenna

The radiation pattern of an array antenna is defined by the array factor (AF) as given in Equation (1):

$$\mathrm{AF} = \sum_{n=0}^{N-1} \boldsymbol{A_n} e^{jn(\beta d \cos\theta)}, \tag{1}$$

where N denotes the number of antenna elements, β is the propagation constant, d is the antenna element spacing and $\boldsymbol{A_n}$ represents the complex excitation signal applied to the nth antenna element. When the amplitude and phase excitations of each antenna element are specified, the array factor yields a unique solution. Under the common assumption that the radiation pattern of an individual antenna element is isotropic, the radiation pattern of the array antenna corresponds to the magnitude of the array factor. Consequently, the relationship between the excitation signals of the antenna elements and the resulting radiation pattern is not one-to-one.

To illustrate this, consider an array antenna composed of eight elements. Figure 1 shows the radiation patterns obtained when the excitation amplitudes of all antenna elements are identical and the phases are sequentially assigned according to the values indicated in the legend. As can be observed, identical radiation patterns can be produced even when different excitation phase configurations are applied to the antenna elements. Although the radiation pattern can be readily computed from the antenna excitation signals using the array factor, it is difficult to inversely estimate the excitation phases of the antenna elements from a given radiation pattern.

Although deep neural networks (DNNs) can be employed to estimate antenna phases from radiation patterns, they generally exhibit limited learning capability when multiple output solutions correspond to a single input. To effectively address this one-to-many mapping problem, a probabilistic artificial intelligence model based on a mixture density network (MDN) is applied to the task of estimating antenna excitation phases from one-dimensional radiation pattern data. The MDN employs the same network architecture as a conventional DNN but outputs the mixture probabilities (π), means (μ), and variances (σ) instead of deterministic values. The MDN is trained such that, in the presence of multiple feasible solutions, the solution associated with the highest probability density is selected.

2.2 | Proposed MDN

The proposed MDN structure is illustrated in Figure 2. The MDN model consists of five hidden layers. The input to the model is a normalised radiation pattern with a maximum value of one, represented by 180 samples corresponding to angles from 0° to 179° with a 1° resolution. The numbers of neurons in the five hidden layers, from the input side to the output side, are 120, 120, 100, 100, and 80, respectively. To compute the radiation pattern

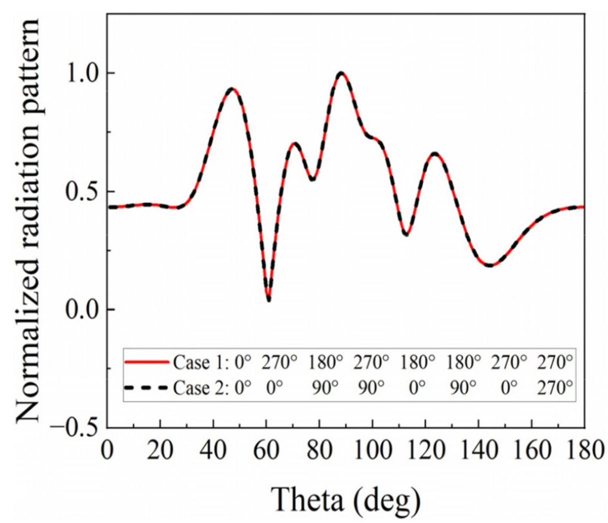

FIGURE 1 | Identical radiation patterns with different phase excitations in an eight-antenna array.

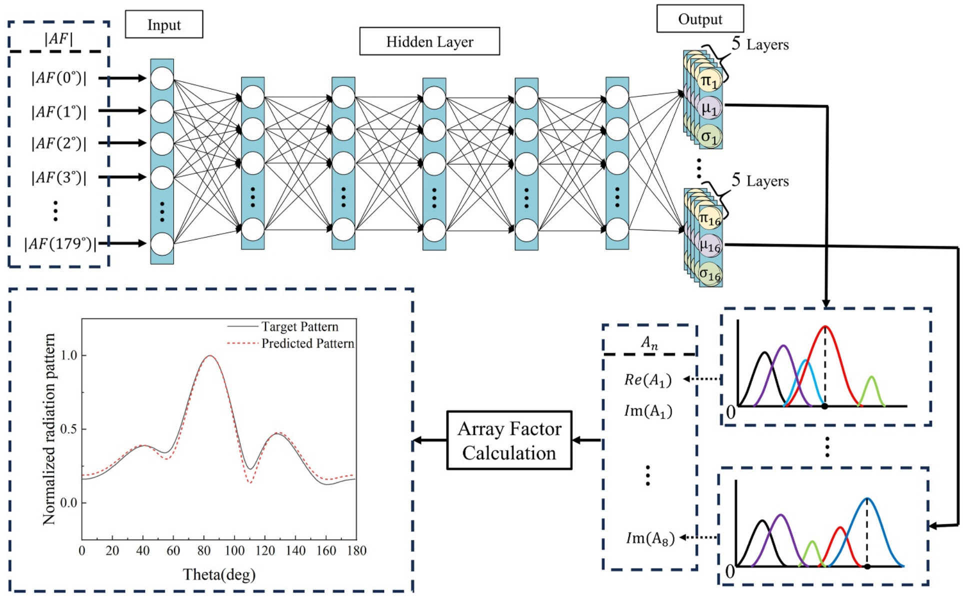

FIGURE 2 | Proposed MDN structure.

from the values predicted by the MDN model, the complex excitation signals applied to each antenna element must be obtained. That is, for each antenna element, either the amplitude and phase or the real and imaginary components of the excitation signal must be estimated. Consequently, a total of 16 values are required to generate a single radiation pattern for the eight-element array antenna. To generate the excitation signal for each antenna element, five probabilistic functions are employed in the MDN. Specifically, the MDN output consists of five sets of mixture probabilities, means, and variances for each of the 16 output variables. For example, to determine the real part of the excitation signal of the first antenna element, ($\mathrm{Re}(A_1)$), the Gaussian component with the highest mixture probability is selected among the five candidate distributions, and its mean value is used as the estimated output.

The primary reason for representing the antenna excitation signals using real and imaginary components rather than phase values is that phase data expressed in angular units introduce discontinuities at 0° and 360° during learning. By expressing the excitation signals in terms of real and imaginary components, the data values are confined to a continuous range between 0 and 1, which is more suitable for neural network training.

The MDN model is trained using a backpropagation algorithm based on gradient descent, which iteratively updates the network weights and biases to minimise the loss function. The negative log-likelihood (NLL) is employed as the loss function for MDN training and is defined as [15].

$$L = -\sum_{n=1}^{N} \ln\left(\sum_{k=1}^{K} \pi_k(x_n) \mathcal{N}\big(y_n \,|\, \mu_k(x_n), \sigma_k(x_n)\big) \right), \tag{2}$$

where N denotes the total number of training samples and K represents the number of Gaussian mixture components, which is set to five. $\mathcal{N}$ denotes the Gaussian probability density function, π_k is the mixture coefficient representing the probability that the kth Gaussian component is selected, μ_k is the mean and σ_k is the variance. The parameters π_k, μ_k and σ_k correspond to the outputs of the MDN. The variables x_n and y_n denote the training data, where x_n is the input one-dimensional radiation pattern vector and y_n is the one-dimensional output vector corresponding to the real and imaginary values of the antenna excitation signals. When the training target y_n is close to the estimated mean μ_k and the corresponding mixture probability π_k is high, the loss function yields a lower value.

The real and imaginary of the antenna excitation signals corresponding to the minimum loss are used to compute the array factor, from which the radiation pattern is derived. The similarity between the derived radiation pattern and the input target radiation pattern is then evaluated to verify the accuracy of the proposed approach.

3 | Comparison Between MDN and DNN

The effectiveness of the proposed MDN approach in estimating the excitation phases of an array antenna for a given target radiation pattern is evaluated. In particular, a comparative analysis with a conventional DNN model is conducted under scenarios where multiple solutions exist for a single radiation pattern.

3.1 | DNN for Comparison

Figure 3 illustrates the DNN model used for performance comparison. The input data consist of the normalised magnitude of the radiation pattern sampled from 0° to 179° with a total of 180 data points. The output data comprise the real and imaginary parts of the excitation signals applied to each antenna element, resulting in a total of 16 output values. Similar to the MDN, the DNN consists of five hidden layers, with the numbers of neurons in each layer set to 120, 120, 100, 100, and 64, respectively. The rectified linear unit (ReLU) is employed as the activation function for all hidden layers, whereas a linear activation function is used for the output layer. All layers are implemented as fully connected (dense) layers.

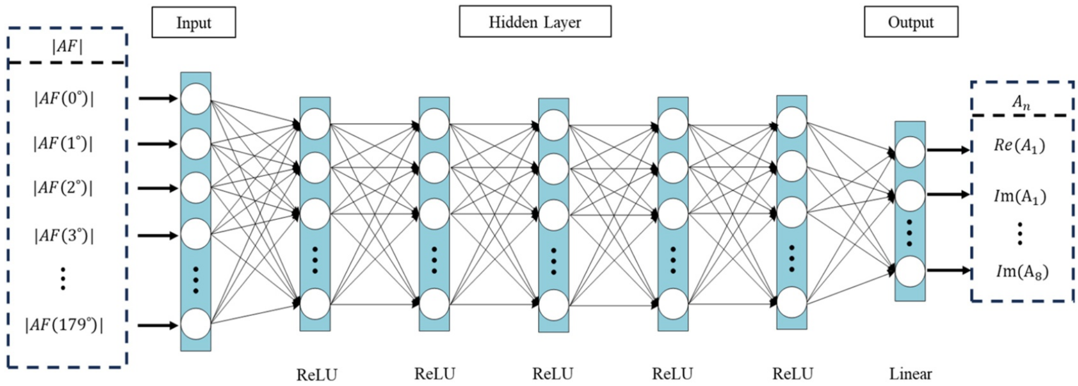

FIGURE 3 | DNN structure.

The mean squared error (MSE) is used as the loss function for model training, and the Adam optimiser is adopted for optimisation.

3.2 | Data Collection and Training

The dataset for training and testing was constructed by computing the AF for an eight-element array antenna. The excitation amplitudes of all antenna elements were fixed to unity. The phase of the first antenna element was fixed at 0°, whereas the phases of the remaining elements (elements 2–8) were varied from 0° to 360° in steps of 90°, resulting in a total of $4^7 = 16,384$ samples.

Although restricting the phase variations to 90° intervals and fixing the amplitude may limit the diversity of the dataset, this design choice was made to prevent the exponential growth of the dataset size. For instance, employing a 30° resolution (12 discrete values per element) for the seven variable elements would require $12^7 = 35,831,808$ samples. Incorporating amplitude variations would further increase the data size exponentially, imposing a significant computational burden in terms of memory and training time. Consequently, the 90° phase interval was selected to avoid difficulties in learning and validation caused by an excessively large dataset. Although this coarse quantisation may affect the initial prediction precision, the proposed iterative retraining framework (discussed in Section 4) effectively overcomes this limitation and improves accuracy, demonstrating the robustness of the algorithm. From the 16,384 samples generated under these settings, 80% were randomly selected for training and the remaining 20% were used for testing.

Each radiation pattern was sampled at 1° intervals and subsequently normalised. As the number of antenna elements increases, the size of the dataset grows exponentially. The models were implemented using the PyTorch framework. The DNN model was trained for 1000 epochs, whereas the MDN model was trained for 2000 epochs. To ensure a fair comparison, both models were optimised using the same baseline settings. The detailed hyperparameter settings for the baseline DNN and the proposed MDN are summarised in Table 1. The loss function values at each epoch are plotted in Figure 4. As shown in the figure, both models exhibit stable convergence behaviour.

TABLE 1 | Hyperparameter setting for the baseline DNN and the proposed MDN.

Parameter	Baseline DNN	Proposed MDN
Optimiser	Adam	Adam
Learning rate	1×10^{-3}	1×10^{-3}
Batch size	512	512
Adam β_1, β_2	0.9, 0.999	0.9, 0.999
Adam ϵ	1×10^{-8}	1×10^{-8}
Loss function	MSE	NLL
Epochs	1000	2000
Number of mixture components (K)	—	5

Furthermore, the rationale for selecting the number of Gaussian mixture components as $K = 5$ is based on a trade-off analysis between prediction accuracy and model complexity. Empirical evaluations demonstrated that $K = 3$ was insufficient to accurately capture the multiple phase solutions. Given that the magnitude and phase of the first antenna element are fixed at 1° and 0°, respectively, it was theoretically anticipated that a maximum of five mixture components would be fully sufficient to represent the required phase combinations. Our simulation results confirmed that $K = 5$ maintains an optimal balance for the 8-element array scenario. Increasing K beyond 5 yielded no meaningful performance improvement, but only increased the computational overhead.

3.3 | Simulation Results

The target radiation pattern was provided as input to the artificial intelligence models to predict the antenna excitation phases, and the predicted phases were subsequently substituted into the array factor formulation to compute the corresponding radiation patterns for comparison. Figure 5 presents a comparison of the radiation patterns predicted by the DNN and the MDN for the radiation pattern shown in Figure 1. The target radiation pattern corresponds to a sample included in the training dataset and is associated with multiple valid output solutions. As expected, the DNN fails to accurately reproduce the target radiation pattern due to its limited capability in learning multiple-output solutions, resulting in a mismatch

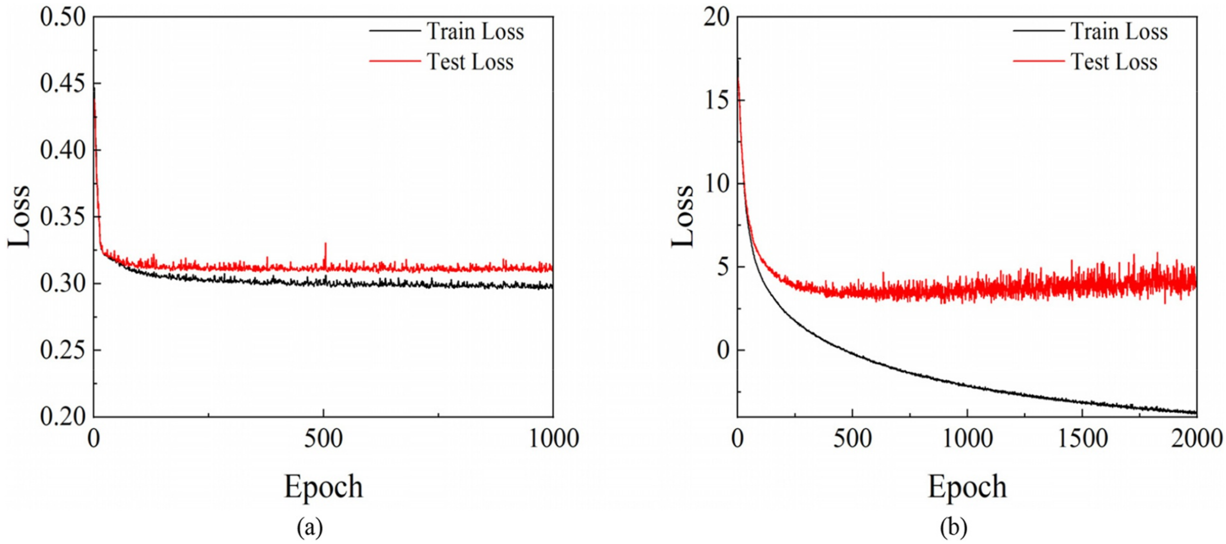

FIGURE 4 | Training and test losses versus epoch: (a) DNN and (b) MDN.

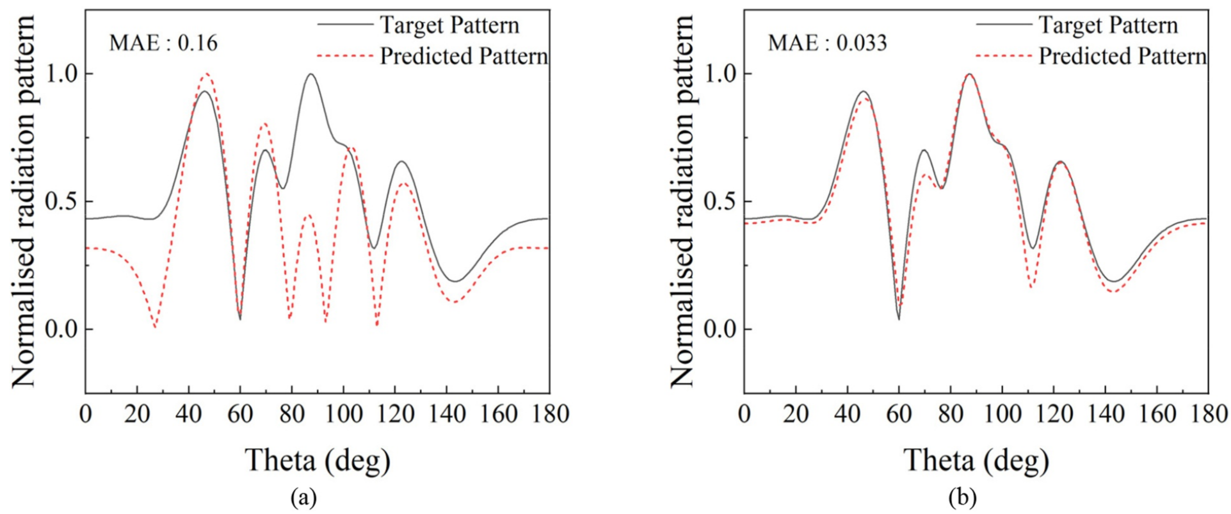

FIGURE 5 | Predicted radiation patterns for the target radiation pattern used as training data: (a) DNN model and (b) MDN model.

between the predicted and target radiation patterns. In contrast, the MDN successfully predicts antenna excitation phases that yield a radiation pattern consistent with the target radiation pattern, despite the presence of multiple feasible solutions.

Figure 6 shows the radiation patterns predicted by the DNN and the MDN when a radiation pattern not included in the training dataset and associated with a unique phase solution is provided as input. The target radiation pattern corresponds to the case in which the excitation phases of all antenna elements are set to 0°. For radiation patterns with a unique phase solution, both algorithms accurately estimate the excitation phases, even though the corresponding patterns are not included in the training dataset.

Figure 7 presents a comparison of phase estimation performance for radiation patterns not included in the training dataset and associated with multiple phase solutions. The target radiation pattern corresponds to the cases in which the excitation phases of the antenna elements are either (0°, 0°, 180°, 0°, 90°, 90°, 90°, 0°) or (0°, 270°, 270°, 270°, 0°, 180°, 0°, 0°). Although neither the DNN nor the MDN perfectly estimates the excitation phases in this scenario, the MDN exhibits relatively more accurate phase estimation performance than the DNN. This limitation is attributed to the insufficient amount of training data as the size of the training dataset increases exponentially with the number of antenna elements, making it impractical to acquire a sufficiently large dataset. To address this issue, Section 4 proposes a data augmentation-based retraining strategy to derive more accurate phase solutions for target radiation patterns.

Furthermore, to ensure the statistical reliability of the results, five independent training runs were conducted using different random seeds. The MAE values presented in Figures 5–7, 9 and 10 represent the mean error across these runs. The statistical variability yielded an overall standard deviation of approximately $\pm\, 0.004$ (relative standard deviation $< 12.5\%$), demonstrating the robust stability of the proposed MDN training process.

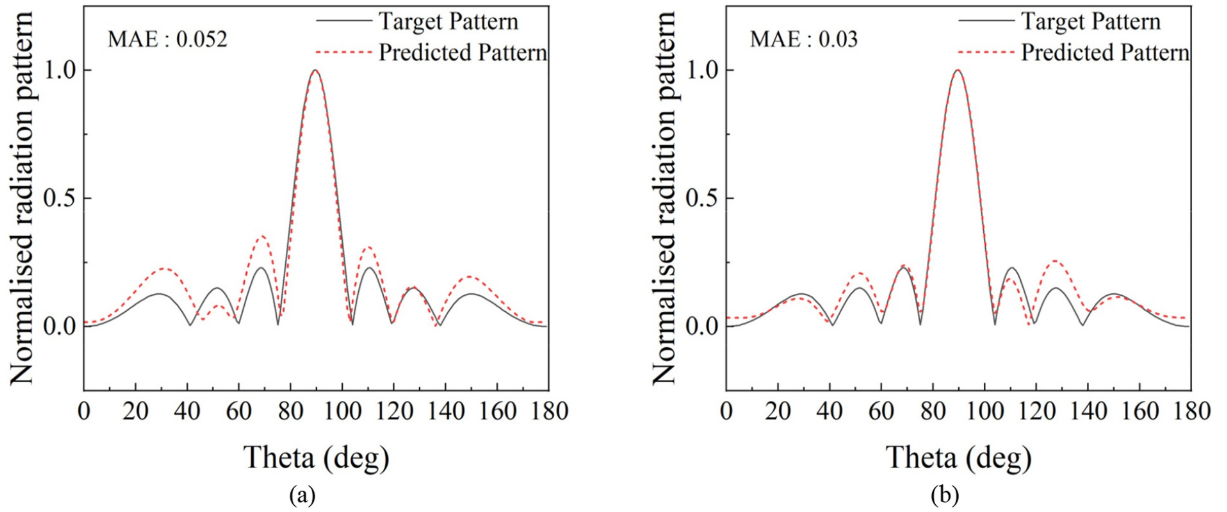

FIGURE 6 | Predicted radiation patterns for an input pattern with a unique solution not included in the training dataset: (a) DNN and (b) MDN.

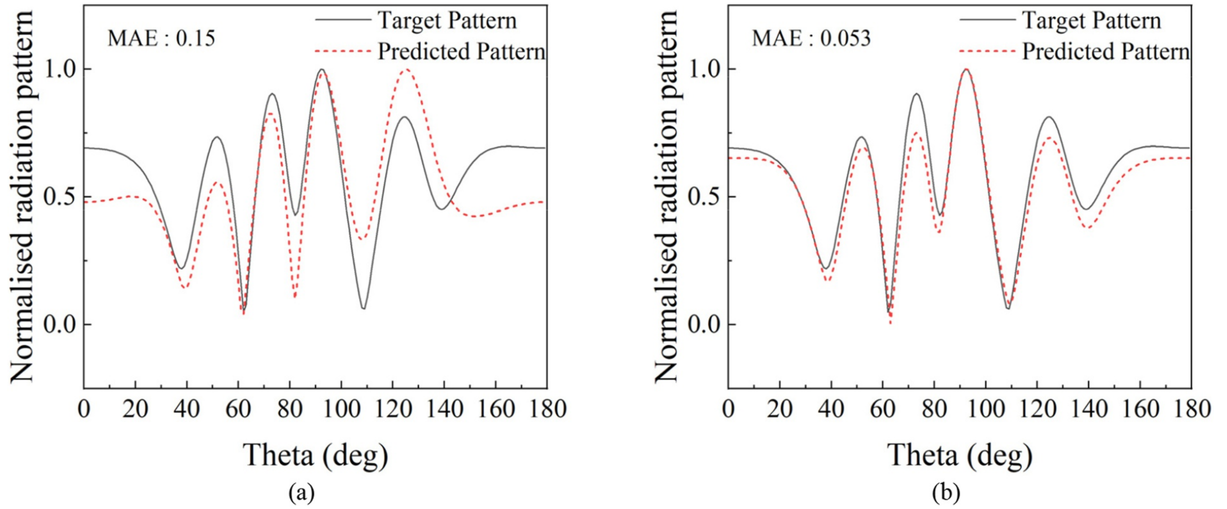

FIGURE 7 | Predicted radiation patterns for an input pattern with multiple solutions not included in the training dataset: (a) DNN and (b) MDN.

4 | Method Using Iterative Retraining

To improve the prediction error that may arise from insufficient initial training data, a data augmentation-based iterative retraining framework is proposed. The specific workflow of the retraining process, which is based on the MAE between the target radiation pattern and the predicted pattern along with a threshold, is defined, and a performance evaluation of the model is conducted for multiple-solution samples not included in the training dataset and arbitrary target patterns that cannot be generated due to the antenna structure.

4.1 | Workflow of the Proposed Iterative Retraining Process

Even if an artificial intelligence model is initially well trained, the initial prediction results may be inaccurate when the amount of training data is insufficient. To address this issue, an iterative retraining process, as illustrated in Figure 8, is proposed.

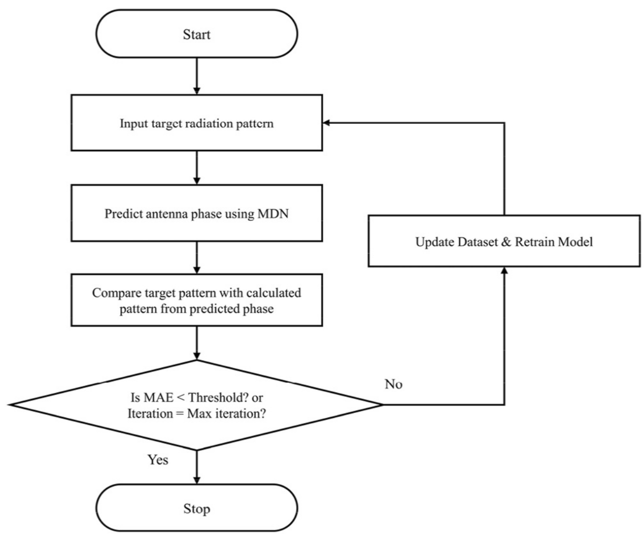

FIGURE 8 | Proposed retraining process.

When a target radiation pattern is provided as input, the MDN model estimates the excitation phases of the array antenna. The predicted phase values are then substituted into the array factor formulation to compute the corresponding radiation pattern. To evaluate the prediction accuracy of the model, the quantitative difference between the input target radiation pattern and the predicted radiation pattern is defined as the mean absolute error (MAE), given by

$$\mathrm{MAE} = \frac{1}{N_s} \sum_{\theta=0^\circ}^{179^\circ} \left| \mathrm{F_t}(\theta) - \mathrm{F_p}(\theta) \right|, \tag{3}$$

where $\mathrm{F_t}(\theta)$ denotes the target radiation pattern as a function of angle, $\mathrm{F_p}(\theta)$ represents the radiation pattern computed from the phase values predicted by the MDN model and N_s represents the total number of angular sampling points ($N_s = 180$). The quantitative difference is calculated based on the mean absolute error (MAE). Each radiation pattern is represented as a scalar-valued function and is normalised such that its maximum value is unity. A threshold value of 0.03 is defined for the MAE to assess the prediction reliability of the model. This threshold was empirically selected through a sensitivity analysis; a tighter threshold (e.g., 0.01) drastically increases computational time with marginal pattern improvement, whereas a looser threshold (e.g., 0.05) compromises prediction accuracy. If the computed MAE is below the threshold, the model is considered to have converged to an optimal solution. Conversely, if the MAE exceeds the threshold, the corresponding data are added to the training dataset, and the model is retrained using the augmented dataset. When the MAE in the current iteration is smaller than that in the previous iteration, 10 additional samples are generated by randomly perturbing the predicted phase values within a range of ± 5° and are used for retraining. If the MAE increases compared to the previous iteration, only the current predicted data point is added to the training dataset. The maximum number of retraining iterations is limited to 50. If the MAE remains above the threshold after reaching the maximum number of iterations, the simulation is terminated.

4.2 | Performance Evaluation

Figure 9 compares the initially predicted radiation pattern and the optimised radiation pattern obtained through the iterative retraining process for a sample not used during training and associated with multiple phase solutions. The radiation pattern predicted prior to retraining, relative to the target radiation pattern, is shown in Figure 9a, whereas the optimised radiation pattern obtained during the retraining iterations is presented in

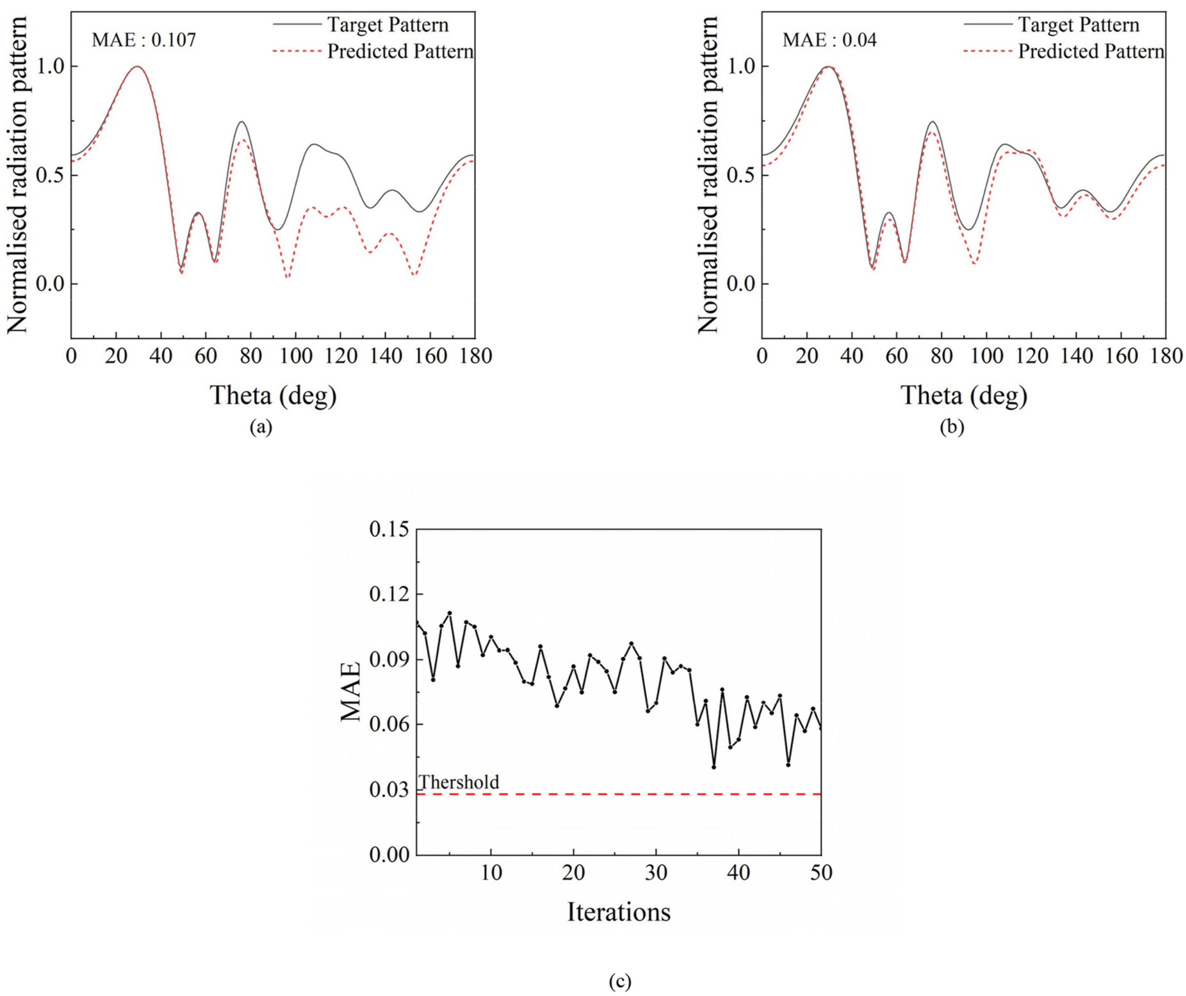

FIGURE 9 | Radiation patterns predicted through the iterative retraining process: (a) initial prediction, (b) optimised radiation pattern within the retraining iterations and (c) error as a function of iteration.

Figure 9b. Figure 9c illustrates the MAE variation over the retraining iterations. At the initial prediction stage, an MAE value of 0.107 was observed. As the retraining process progressed, the MAE gradually decreased, reaching a minimum value of 0.04. These results demonstrate that the MDN successfully identifies appropriate phase solutions through iterative feedback, thereby confirming the effectiveness of the proposed retraining framework.

Figure 10 illustrates how the proposed MDN model with iterative retraining estimates radiation patterns for an arbitrary target radiation pattern that cannot be generated using an eight-element array antenna. Figure 10a shows the radiation pattern predicted at the initial inference stage, for which the MAE is 0.275. Figure 10b presents the radiation pattern optimised through the retraining process, with a corresponding MAE of 0.113. At this time, the excitation phases applied to each antenna element are (0°, 10.5°, 34.44°, −135.69°, −146.91°, 140.9°, 35.6° and −117.28°). Although the MAE does not decrease below the threshold value of 0.03 during the retraining stage, the proposed method successfully derives antenna excitation phase values that yield the radiation pattern most similar to the target pattern within the considered range.

Table 1 summarises previous studies that applied artificial intelligence techniques for radiation pattern synthesis. Most existing ANN- or DNN-based array synthesis methods assume a deterministic one-to-one mapping between the radiation pattern and the excitation parameters. Consequently, their performance degrades when multiple valid solutions exist for a single radiation pattern. In contrast, the proposed method employs a mixture density network (MDN) to explicitly model the conditional probability distribution of antenna excitations, enabling effective learning in the presence of nonunique inverse solutions.

As clearly demonstrated in the updated Table 2, our proposed MDN framework exhibits overwhelming advantages in computational efficiency. Although recurrent architectures. such as the GRU, in ref. [17] require a massive number of trainable parameters (e.g., 6.63×10^6) leading to significant computational overhead, our MLP-based MDN is highly

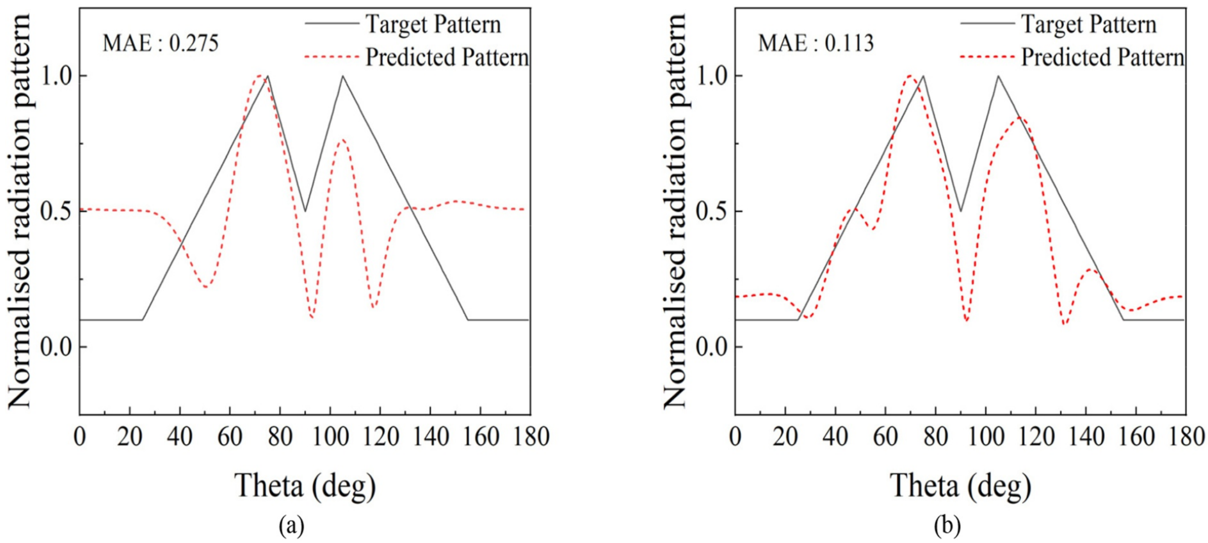

FIGURE 10 | Predicted radiation patterns for an arbitrary target radiation pattern: (a) initial prediction and (b) optimised radiation pattern within the retraining iterations.

TABLE 2 | Comparison of previous studies on radiation pattern synthesis using artificial intelligence.

Ref	Array geometry	Input	Output	AI method	Training data size	Inference time (s)	Trainable parameters	Multisolution
[7]	1 × 8 array	Radiation characteristics	Antenna excitations	ANN	N/A	N/A	$\sim 2.15 \times 10^4$	X
[9]	1 × 4 array	Radiation pattern	Antenna excitations	DNN	40,000	N/A	$\sim 6.3 \times 10^4$	X
[10]	1 × 50 array	Mask-constrained beampattern	Antenna excitations	Encoder–decoder ANN	100,000	N/A	$\sim 3.86 \times 10^4$	X
[17]	1 × 8 array	Radiation pattern	Antenna excitations	GRU	7623	0.036	6.63×10^6	X
This work	1 × 8 array	Radiation pattern	Antenna excitations	MDN	16,384	3.7×10^{-4}	9.57×10^4	O

lightweight, requiring only 9.57×10^4 parameters and achieving an extremely fast inference time of 3.7×10^{-4} s. Most importantly, despite its remarkably low computational cost, our MDN uniquely resolves the 'multi-solution (non-uniqueness)' problem by outputting a continuous probability distribution, without relying on data-filtering preoptimisation. Furthermore, although Table 2 provides a comprehensive comparison of computational complexity, it should be noted that a direct comparison of prediction errors, such as RMSE, across all methods is practically difficult. This is because each referenced study utilises fundamentally different datasets, array configurations and evaluation scenarios. Nevertheless, the proposed MDN effectively achieves the desired radiation pattern synthesis with reliable precision.

It is worth noting the computational overhead associated with the proposed framework. As detailed in Table 2, the MDN inference after initial training is extremely efficient, taking only 0.37 ms per pattern on a GPU. However, the iterative retraining process introduces additional latency, with each retraining iteration taking approximately 60 seconds. Consequently, the worst-case scenario requiring the maximum of 50 iterations takes up to 3000 seconds. This timeframe is well within acceptable limits for offline array synthesis tasks.

5 | Conclusion

In this paper, a mixture density network (MDN)-based approach combined with a retraining strategy is proposed for array antenna radiation pattern synthesis. Unlike conventional deep neural networks (DNNs), which predict a single solution for a given input, the proposed MDN estimates the probability distribution of solutions, enabling effective learning even when a one-to-one correspondence between the radiation pattern and antenna excitation phases does not exist. The performance of the proposed MDN was evaluated through a comparative study with a conventional DNN using an eight-element array antenna. The results show that the MDN provides more accurate phase estimation than the DNN for radiation patterns associated with multiple phase solutions. Furthermore, by introducing an iterative retraining scheme that incrementally augments the training dataset for arbitrary target radiation patterns, the proposed method successfully identifies radiation patterns that closely match the desired targets. The proposed approach is expected to be applicable to a wide range of antenna design problems involving multiple feasible solutions.

Although the proposed framework has been successfully validated for an eight-element array, extending this approach to large-scale arrays (e.g., 16, 32, or 64 elements) offers promising avenues for future research. As the array size increases, the required dataset size grows exponentially (M^{N-1}). To efficiently manage this dataset scalability and multiple phase solutions in massive MIMO arrays, future work will integrate advanced data generation strategies, such as active learning, along with careful architectural optimisations including the systematic scaling of Gaussian mixture components (K). Moreover, future studies will focus on developing mechanisms to predetect physically unrealisable patterns prior to inference. To address the limitations of phase-only control, future work will also expand the model for joint amplitude-phase optimisation by integrating amplitude variables directly into the localised retraining stage, thereby avoiding an exponential explosion of the initial training dataset. Finally, to mitigate retraining latency for real-time applications, future optimisation strategies will explore transfer learning, early-stopping mechanisms, and precomputed look-up libraries.

Author Contributions

Je-Heon Lee: conceptualisation, data curation, formal analysis, investigation, methodology, software, validation, visualisation, writing – original draft, writing – review and editing. **Hyeon-Chang Seong:** data curation, formal analysis, methodology, validation. **Jungsuek Oh:** data curation, formal analysis, funding acquisition, validation. **Jae Hee Kim:** funding acquisition, project administration, resources, supervision, writing – review and editing.

Acknowledgements

This work was supported by the Institute of Information and communications Technology Planning and Evaluation (IITP) grant funded by the Korea government (MSIT) (Grant RS-2021-II210763, Innovative Fusion Technologies of Intelligent Antenna Material/Structure/Network for THz 6G).

Conflicts of Interest

The authors declare no conflicts of interest.

Data Availability Statement

Research data are not shared.

References

1. C. A. Balanis, *Antenna Theory: Analysis and Design*. 4th ed. (Wiley, 2016).

2. J. D. Kraus, *Antennas*. 2nd ed. (McGraw-Hill, 1988).

3. D. W. Boeringer, D. H. Werner, and D. W. Machuga, "A Simultaneous Parameter Adaptation Scheme for Genetic Algorithms With Application to Phased Array Synthesis," *IEEE Transactions on Antennas and Propagation* 53, no. 1 (January 2005): 356–371, https://doi.org/10.1109/TAP.2004.838800.

4. L. Manica, N. Anselmi, P. Rocca, and A. Massa, "Robust Mask-Constrained Linear Array Synthesis Through an Interval-Based Particle Swarm Optimisation," *IET Microwaves, Antennas & Propagation* 7, no. 12 (September 2013): 976–984, https://doi.org/10.1049/iet-map.2013.0203.

5. D. G. Kurup, M. Himdi, and A. Rydberg, "Synthesis of Uniform Amplitude Unequally Spaced Antenna Arrays Using the Differential Evolution Algorithm," *IEEE Transactions on Antennas and Propagation* 51, no. 9 (September 2003): 2210–2217, https://doi.org/10.1109/TAP.2003.816361.

6. H. Bilel, L. Selma, and A. Taoufik, "Artificial Neural Network (ANN) Approach for Synthesis and Optimization of (3D) Three-Dimensional Periodic Phased Array Antenna," in *2016 17th International Symposium on Antenna Technology and Applied Electromagnetics (ANTEM)*, (IEEE, 2016), 1–6, https://doi.org/10.1109/ANTEM.2016.7550118.

7. L. Merad, F. T. Bendimerad, S. M. Meriah, and S. A. Djennas, "Neural Networks for Synthesis and Optimization of Antenna Arrays," *Radioengineering* 16, no. 1 (April 2007): 70–74.

8. X. Xiao and Y. Lu, “Data-Based Model for Wide Nulling Problem in Adaptive Digital Beamforming Antenna Array,” *IEEE Antennas and Wireless Propagation Letters* 18, no. 11 (November 2019): 2259–2263, https://doi.org/10.1109/LAWP.2019.2925419.

9. J. H. Kim and S. W. Choi, “A Deep Learning-Based Approach for Radiation Pattern Synthesis of an Array Antenna,” *IEEE Access* 8 (2020): 226059–226063, https://doi.org/10.1109/ACCESS.2020.3045464.

10. C. Cui, W. T. Li, X. T. Ye, P. Rocca, Y. Q. Hei, and X. W. Shi, “An Effective Artificial Neural Network-Based Method for Linear Array Beampattern Synthesis,” *IEEE Transactions on Antennas and Propagation* 69, no. 10 (October 2021): 6431–6443, https://doi.org/10.1109/TAP.2021.3069467.

11. C. Niu, M. Phaneuf, T. Qiu, and P. Mojabi, “A Deep Learning-Based Approach to Design Metasurfaces From Desired Far-Field Specifications,” *IEEE Open Journal of Antennas and Propagation* 4 (2023): 641–653, https://doi.org/10.1109/OJAP.2023.3292108.

12. J. Zhou, H. Xia, Y. Wang, X. Bai, W. Zhang, and R. Yang, “Deep Conditional Generative Adversarial Network-Assisted Inverse Design of Metasurface,” in *2024 International Applied Computational Electromagnetics Society Symposium (ACES-China)*, (2024), 1–3, https://doi.org/10.1109/ACES-China62474.2024.10700005.

13. Z. Liu, D. Zhu, S. P. Rodrigues, K-T. Lee, and W. Cai, “Generative Model for the Inverse Design of Metasurfaces,” *Nano Letters* 18, no. 10 (September 2018): 6570–6576, https://doi.org/10.1021/acs.nanolett.8b03171.

14. S. An, B. Zheng, M. Shalaginov, et al., “Deep Learning Modeling Approach for Metasurfaces With High Degrees of Freedom,” *Optics Express* 28, no. 21 (October 2020): 31932–31942, https://doi.org/10.1364/OE.401960.

15. C. M. Bishop, *Mixture Density Networks*, Technical Report NCRG/94/004 (Aston University, 1994).

16. R. Unni, K. Yao, and Y. Zheng, “Deep Convolutional Mixture Density Network for Inverse Design of Layered Photonic Structures,” *ACS Photonics* 7, no. 10 (September 2020): 2703–2712, https://doi.org/10.1021/acsphotonics.0c00630.

17. A. Arce, F. Arce, E. Stevens-Navarro, U. Pineda-Rico, M. R. Rahmati, and A. García-Barrientos, “GRU-Based Beam Pattern Synthesis for Optimized Uniform Linear Antenna Arrays,” *Informatics* 13, no. 4 (April 2026): 60, https://doi.org/10.3390/informatics13040060.